Journal of the Optical Society of Korea, Vol 5, No. 3, September 2001, pp. 76-82

Optical Response of Traveling-Wave Optical Modulator with 3-Section Phase Reversal

Chang-Min Kim* and Young-Tak Han

Dept. of Electronics Engineering, The University of Seoul, Seoul 130-743, KOREA

(Received April 19, 2001)

The optical response for traveling-wave Mach-Zehnder modulators without/with phase reversal is successfully derived in more concise and succinct form than any other equations before. The obtained equation is applied to a bandpass traveling-wave modulator with 3-section phase reversal and is confirmed to be in reasonable agreement with the experimental data.

OCIS codes : 230.4110, 230.7020, 250.7360.

I. INTRODUCTION

High-speed optical modulator is an indispensible component in high-capacity and wide-band optical communication systems and its application is extended to optical switching, sampling, and signal processing. The optical modulators consist of optical waveguide/coupler and traveling-wave electrodes. The waveguides are fabricated by diffusing Ti in $LiNbO_3$ crystal with high electrooptic coefficient and the coplanar waveguide (CPW) electrodes are built on waveguides to control the optical switching.

The high-speed performance of the traveling-wave optical modulator is limited by the following three factors [1–8]:

i) propagation velocity mismatch between optical wave (OW) and modulating microwave (MW)

ii) MW loss in traveling-wave electrodes

iii) Impedance mismatch between MW driver and traveling electrodes

Several ways to overcome the above limiting factors have been successfully presented as follows : First, thick electrodes, most part of which is exposed to the air, are employed to lower the MW effective index 4.2 of bulk $LiNbO_3$ down to the optical effective index 2.2, thus achieving the velocity match. This thick structure also guarantees low loss in MW propagation. However, it is difficult to achieve both velocity and impedance match simultaneously with this recipe only. Second, SiO_2 buffer layer is introduced to aim at reducing TM mode propagation loss of guided optical wave and, by controlling the thickness of this layer, designers can afford to acquire velocity match/impedance match. Third, use of thin $LiNbO_3$ eliminates the occurrence of MW substrate mode to obtain wider-band optical response.

Thanks to the efforts of many researchers, the bandwidth of traveling-wave modulators has been increased up to more than 50 GHz recently [6,7]. Traveling-wave modulators above 30 GHz becomes easily available and general curves of optical response show typical trend that drops down to -3 dB over 0~few tens of GHz.

On the other hand, with the development of subcarrier multiplexing (SCM) technology in optical communication, there arise needs for the high-speed optical modulator with a bandpass characteristics [9–14]. Therefore, optical modulators do not need to have almost flat frequency response over the band ranging from 0 to tens of GHz. In SCM systems, the optical modulator may show flat response only in a pass-band with a center frequency of subcarrier. This kind of optical modulators can be achieved in optical guiding structure with phase-reversal characteristics. As the phase reversed traveling-wave modulators may have a bandpass filter characteristics under a certain degree of velocity mismatching [15] only, designers have more rooms in designing electrodes' structure than before once a bandwidth and a center frequency are given. In conventional high-speed modulators, design of electrodes have been usually difficult to implement since both the velocity matching and the impedance matching need to be met at the same time.

In this work, we investigate the frequency response

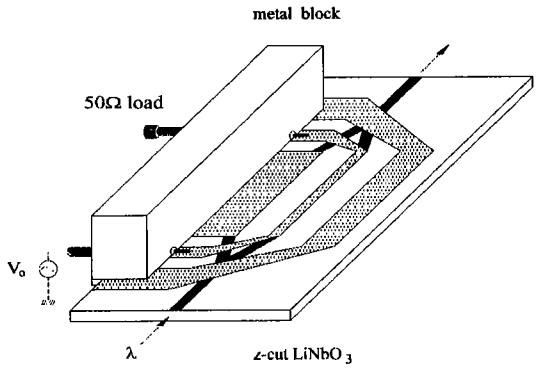

FIG. 1. Schematic diagram of a traveling-wave optical modulator.

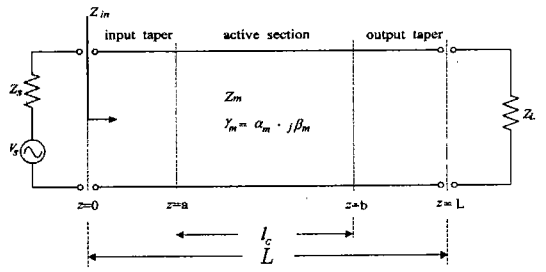

FIG. 2. Equivalent transmission line of travelling-wave electrodes. l_c : Interaction length between optical wave and MW. L : Overall length of MW electrodes.

of the traveling-wave optical modulator fabricated on z-cut Ti:$LiNbO_3$ waveguide with 3-section phase reversal. Theoretical analysis is performed for the modulator which was designed and fabricated by Ramaswamy [9]. The fabrication process of the device is summarized as follows : First, they made 3-sectioned reversed domains by the electric-field polling technique on z-cut $LiNbO_3$ substrate, on which Ti-indiffused optical waveguide and Mach-Zehnder (M-Z) interferometer were fabricated. SiO_2 buffer layer was deposited on the surface, followed by building up CPW electrodes by use of the electrolyte technique. Experimental results showed that the device had a bandpass filter characteristics as expected, but the theoretical estimation was performed rather vaguely.

In our analytical process, traveling-wave electrodes are modelled as a transmission line and the voltage distribution is represented as the sum of forward traveling-wave and backward traveling-wave. The relative voltage distribution with respect to a guided optical beam is derived and the overall index change along waveguides due to the impressed MW voltage is also expressed in integral form. The modulation bandwidth, or response speed is represented as a function of velocity mismatch, impedance mismatch and MW propagation loss. It turns out that our simulation results are in good agreement with the experimental results.

II. OPTICAL RESPONSE OF TRAVELING-WAVE MODULATORS

In Fig. 1(a) traveling-wave optical modulator composed of M-Z interferometer and CPW electrodes is illustrated.

To quantify the modulation bandwidth of the optical modulator as a function of MW characteristic impedance Z_m, the MW effective index N_{eff} and the optical effective index n_{eff}, the MW electrodes is modelled as an equivalent transmission line as shown in Fig. 2.

In Fig. 2, V_s and Z_s denote the MW source and the characteristic impedance of a feeding coaxial cable. Z_m and Z_L represent characteristic impedances of electrodes and of a terminal load, respectively. γ_m means the propagation constant, where α_m, β_m are the attenuation constant and the phase constant, respectively.

Distributed voltage $V(z)$ along the transmission line is represented as the sum of the forward traveling-wave and the backward traveling-wave, the term $\exp(j\omega t)$ is omitted for convenience's sake.

$$V(\omega_m, z) = V_s \frac{Z_{in}}{Z_{in}+Z_s} \cdot \frac{1}{1+\Gamma_L \exp(-2\gamma_m L)} \left[\exp(-\gamma_m z) + \Gamma_L \exp(-2\gamma_m L)\exp(\gamma_m z) \right] \quad (1)$$

where

$$\Gamma_L = (Z_L - Z_m)/(Z_L + Z_m) \quad : \text{Reflection coeff.} \quad (2)$$

$$\gamma_m(\omega_m) = \alpha_m + j\beta_m \quad : \text{MW prop. const.} \quad (3)$$

$$Z_{in}(\omega_m) = Z_m \frac{Z_L + Z_m \tanh(\gamma_m L)}{Z_m + Z_L \tanh(\gamma_m L)} \quad : \text{Input impedance} \quad (4)$$

Guided light propagating along an optical waveguide is electrooptically influenced by the MW traveling along the electrodes placed above. Eq. (1) is the

impressed voltage of traveling MW along the z-axis and needs to be modified to a relative expression seen by the guided light's standpoint. Let us put the expression of forward-traveling MW in a simple form as below for brief discussion.

$$\text{MW} : V(\omega_m, z) = \exp(-j\beta_m z) = \exp(-j\frac{\omega_m}{c}z) = \exp(-j\frac{\omega_m}{c_0}N_{eff}z) \tag{5}$$

c_0 is the light velocity in vacuum. The relative voltage from the view of guided light may be expressed as [1]

$$\text{MW} : V'(\omega_m, z) = \exp(-j\frac{\omega_m}{c}(N_{eff} - n_{eff})z) = V(\omega_m, z)/\exp(-j\frac{\omega_m}{c_0}n_{eff}z) \tag{6}$$

When we consider that the division process of Eq. (6) holds for a backward-traveling wave as well, Eq. (1) needs to be divided by the phase expression of $\exp(-j\frac{\omega_m}{c_0}n_{eff}z)$. The relative distributed votage $V'(z)$ along the transmission line is now

$$\begin{aligned} V'(\omega_m, z) &= V(\omega_m, z)/\exp(-j\frac{\omega_m}{\omega_0}\beta_0 z) \\ &= V_s\frac{Z_{in}}{Z_{in}+Z_s}\frac{1}{1+\Gamma_L\exp(-2\gamma_m L)}\left[\exp(p^+z) + \Gamma_L\exp(-2\gamma_m L)\exp(p^-z)\right] \end{aligned} \tag{7}$$

where

$$p^+ = -\alpha_m - j\frac{\omega_m}{c_0}(N_{eff} - n_{eff}) \tag{8}$$

$$p^- = \alpha_m + j\frac{\omega_m}{c_0}(N_{eff} + n_{eff}) \tag{9}$$

Specially at $\omega_m = 0$, $V'(0, z)$ becomes constant throughout the electrodes,

$$V'(0, z) = V_s\frac{Z_L}{Z_L + Z_s} \tag{10}$$

since

$$Z_{in} = Z_L, \quad \Gamma_L = 0, \quad p^{\pm} = 0. \tag{11}$$

On the other hand, $\overline{\Delta n}(\omega_m)$, the overall index change occurred in the active section, may be expressed in case of z-cut $LiNbO_3$ waveguide devices.

For electrodes without phase reversal, $\overline{\Delta n}(0)$ and $\overline{\Delta n}(\omega_m)$ are written to be

$$\overline{\Delta n}(0) = c_{eo}\left|\int_a^b V'(0, z)dz\right| = c_{eo}\left|V_s\frac{Z_L}{Z_L+Z_s}(b-a)\right| \tag{12}$$

$$\overline{\Delta n}(\omega_m) = c_{eo}\left|\int_a^b V'(\omega_m, z)dz\right| = c_{eo}\left|V_s\frac{Z_{in}}{Z_{in}+Z_s}\frac{1}{1+\Gamma_L\exp(-2\gamma_m L)}\int_a^b g(\omega_m, z)dz\right| \tag{13}$$

where

$$g(\omega_m, z) = \exp(p^+z) + \Gamma_L\exp(-2\gamma_m L)\exp(p^-z) \tag{14}$$

$$c_{eo} = \frac{1}{2}n_{eff}^3\gamma_{33}\Gamma\frac{1}{S} \tag{15}$$

The distance between a and b is the section length of interaction between MW and OW. γ_{33}, Γ and S is the electrooptic coefficient, the overlap integral factor, and the gap between electrodes, respectively. The coefficient c_{eo} is a proportional constant of electrooptic effect. $\Delta n(0)$ is the index change by impressed dc voltage for switching.

For electrodes with phase reversal of odd numbers, $\overline{\Delta n}(0)$ and $\overline{\Delta n}(\omega_m)$ are expressed as

$$\begin{aligned} \overline{\Delta n}(0) &= c_{eo}\left|\int_a^{a+h} V'(0, z)dz - \int_{a+h}^{a+2h} V'(0, z)dz + \int_{a+2h}^{a+3h}\cdots\int_{b-h}^{b} V'(0, z)dz\right| \\ &= c_{eo}\left|V_s\frac{Z_L}{Z_L+Z_s}h\right| \end{aligned} \tag{16}$$

$$\overline{\Delta n}(\omega_m) = c_{eo}\left|\int_a^{a+h} V'(\omega_m,z)dz - \int_{a+h}^{a+2h} V'(\omega_m,z)dz + \int_{a+2h}^{a+3h}\cdots\int_{b-h}^{b} V'(\omega_m,z)dz\right|$$
$$= c_{eo}\left|V_s\frac{Z_{in}}{Z_{in}+Z_s}\frac{1}{1+\Gamma_L\exp(-2\gamma_m L)}\left[\int_a^{a+h} g(\omega_m,z)dz - \int_{a+h}^{a+2h} g(\omega_m,z)dz\right]\right| \quad (17)$$

where

$$h = \frac{b-a}{m} \quad (18)$$

From Eq. (12) through Eq. (17), the ratio of $\overline{\Delta n}(\omega_m)$ with respect to $\overline{\Delta n}(0)$ becomes

i) For electrodes without phase reversal ;

$$\frac{\overline{\Delta n}(\omega_m)}{\overline{\Delta n}(0)} = \left|\frac{Z_{in}}{Z_L}\frac{Z_L+Z_s}{Z_{in}+Z_L}\frac{1}{(b-a)(1+\Gamma_L\exp(-2\gamma_m L))}\int_a^b g(\omega_m,z)dz\right| \quad (19)$$

ii) For electrodes with m-section phase reversal ;

$$\frac{\overline{\Delta n}(\omega_m)}{\overline{\Delta n}(0)} = \left|\frac{Z_{in}}{Z_L}\frac{Z_L+Z_s}{Z_{in}+Z_L}\frac{m}{(b-a)(1+\Gamma_L\exp(-2\gamma_m L))}\left[\int_a^{a+h} g(\omega_m,z)dz - \int_{a+h}^{a+2h} g(\omega_m,z)dz\cdots\int_{b-h}^{b} g(\omega_m,z)dz\right]\right| \quad (20)$$

Referring to the optical response $R(\omega_m)$ defined and derived in Appendix A, $R(\omega_m)$ is described as

$$R(\omega_m) = \left|\sin\left(\frac{\pi}{2}\frac{\overline{\Delta n}(\omega_m)}{\overline{\Delta n}(0)}\right)\right| \quad (21)$$

Insertion of Eq. (19) or (20) into Eq. (21) leads us to the optical response.

III. ESTIMATION AND MEASUREMENT OF OPTICAL RESPONSE

Based on the developed equations, we perform the analysis of a bandpass traveling-wave M-Z modulator on a 0.5 mm-thick z-cut $LiNbO_3$ substrate, which was experimentally demonstrated by Ramaswamy et al. The fabricated modulator consisted of a symmetrical M-Z interferometer with 4 μm-wide optical waveguide arms and a CPW type electrode as in Fig. 3.

The total electrode length L including the input/output tapers was 2.4 cm long. The interaction length l_c was chosen to be 1 cm long, which was again partitioned into 3 parts by the domain-reversal.

Measured S-parameter curves are illustrated in Fig. 4.

The procedure to obtain parameters N_{eff}, α_0 and Z_m are briefly described below.

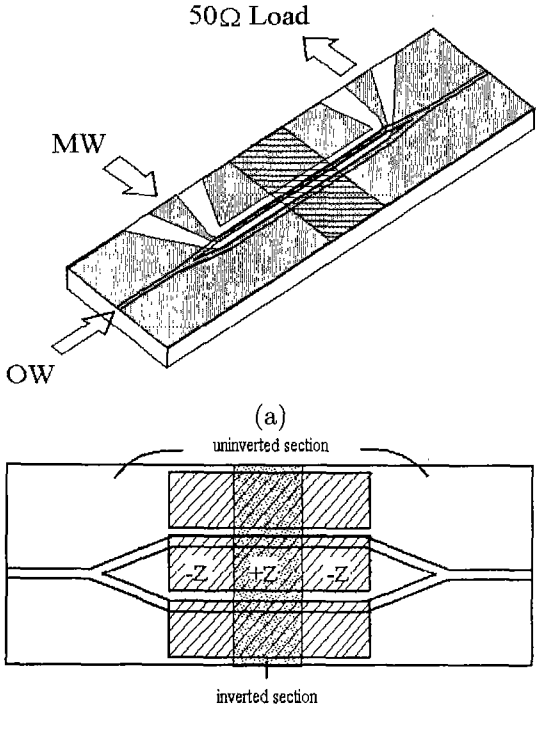

FIG. 3. Traveling-wave M-Z modulator with 3-section domain reversal. (a) Overview of traveling-wave M-Z modulator. (b) Detailed view of CPW electrodes with 3-section domain reversal.

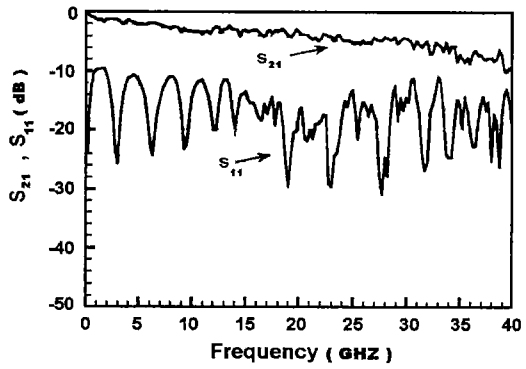

FIG. 4. Measured S-parameter curves.

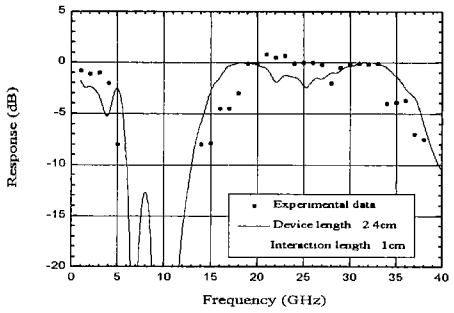

FIG. 5. Frequency response of traveling-wave M-Z modulator with 3-section domain reversal ($\lambda = 1.32\ \mu m$, $n_{eff} = 2.148$, $N_{eff} = 3.7$, $\alpha_0 = 0.4$ dB/cm $\cdot \sqrt{\text{GHz}}$, $Z_{in} = 35\ \Omega$, $Z_s = Z_L = 50\ \Omega$).

1. Microwave effective index N_{eff}

   N_{eff} is deduced from the equation

$$N_{eff} = \frac{c_0}{2L\Delta f} \tag{22}$$

   c_0 is the light velocity in vacuum and L is the electrode's total length.

   Δf is the frequency gap between two neighboring dips on the S_{11} curve.

2. Microwave loss coefficient α_0

   α_0 is extracted from the attenuation slope on the S_{21} curve.

$$\alpha_m = \alpha_0 \sqrt{f(\text{in GHz})}\text{cm}^{-1} \tag{23}$$

   The conversion rule between neper and dB is

$$\alpha_0 = \alpha_0(\text{dB})/8.686 \tag{24}$$

3. Characteristic impedance Z_m

   Z_m can be figured out from the peak of first lobe on the S_{11} curve.

   Z_{in} is calculated from the S_{11}, rendering Z_m.

4. Optical refractive index n_{eff}

   $n_{eff} = 2.148$ at $\lambda = 1.32\ \mu m$

From the observation of S-parameters' curves of Fig. 4, the following data are obtained.

$$N_{eff} = 3.7,\ \ \alpha_0 = 0.4\ \text{dB/cm} \cdot \sqrt{\text{GHz}},\ \ Z_{in} = 35\ \Omega \tag{25}$$

The acquired data of Eq. (25) are inserted in Eqs. (20) and (21) to estimate the frequency response curve. The response of the modulation is illustrated in Fig. 5, where the theoretical curve is plotted for comparison with the experimental data.

As seen from Fig. 5, the experimental result is in reasonable agreement with the theoretical expectation. In the simulation, a straight transmission line of constant impedance was assumed and, therefore, the MW reflection spatially distributed along the tapers and bends of electrodes was not considered for in the calculation. We attribute the difference between the experiment and the theory to ignoring reflection phenomenon in tapers and bends.

IV. CONCLUSIONS

The optical response for traveling-wave M-Z modulators without/with phase reversal is defined and is successfully derived in more concise and succinct form than any other equations before. The algorithm used in the derivation can be equally applied to any type of modulators including directional coupler type. The modulation bandwidth, or response speed is represented as a function of velocity mismatch, impedance mismatch and MW propagation loss. The obtained equation is applied to a bandpass traveling-wave modulator with 3-section phase reversal and the calculated results are confirmed to be in fairly good agreement with the experimental data.

V. ACKNOWLEDGEMENTS

This work was supported by the 2000 University Research Program, Ministry of Information and Communication, and by the 2000 Research Foundation, Ministry of Education.

APPENDIX A. OPTICAL RESPONSE OF M-Z MODULATOR

When the switching operation is performed, the propagation constants' difference between two waveguides $\Delta\beta(\omega_m)$ at the index difference $\overline{\Delta n}(\omega_m)$ satisfy the following relations.

$$\Delta\beta(0)\cdot l_c = \pi \quad \text{bias for full swing} \tag{A.1}$$

$$\Delta\beta(\omega_m) \simeq k_0\overline{\Delta n}(\omega_m) \tag{A.2}$$

The optical response $R(\omega_m)$ in terms of optical output intensity $I(\omega_m)$ is defined as

$$R(\omega_m) \equiv \sqrt{\frac{I(\omega_m) - I_{\phi_0}}{I(0) - I_{\phi_0}}} \tag{A.3}$$

where the optical output intensity $I(\omega_m)$ is

$$\begin{aligned} I(\omega_m) &= \left|\frac{1}{2}\exp[-j(\beta_1(\omega_m)l_c + \phi_0)] + \frac{1}{2}\exp[-j(\beta_2(\omega_m)l_c - \phi_0)]\right|^2 \\ &= \cos^2\left(\frac{\Delta\beta(\omega_m)l_c}{2} + \phi_0\right) \end{aligned} \tag{A.4}$$

where $\Delta\beta = \beta_1 - \beta_2$.

ϕ_0 is optical bias point. Now that the power output is always unity when no voltage is applied to symmetric M-Z interferometer, $I_{\phi_0} = 1$. Then the optical intensity response $R(\omega_m)$ is

$$R(\omega_m) = \left|\frac{\cos^2\frac{\Delta\beta(\omega_m)l_c}{2} - 1}{\cos^2\frac{\Delta\beta(0)l_c}{2} - 1}\right|^{1/2} = \left|\frac{\sin\frac{\Delta\beta(\omega_m)l_c}{2}}{\sin\frac{\Delta\beta(0)l_c}{2}}\right| \tag{A.5}$$

Substituting the condition of Eq. (A1), $R(\omega_m)$ renders to

$$R(\omega_m) = \sin\left(\frac{\pi}{2}\left|\frac{\Delta\beta(\omega_m)}{\Delta\beta(0)}\right|\right) \approx \sin\left(\frac{\pi}{2}\left|\frac{\overline{\Delta n}(\omega_m)}{\overline{\Delta n}(0)}\right|\right) \tag{A.6}$$

APPENDIX B. INDIRECT MEASUREMENT TECHNIQUE BY USING A SLOW-SPEED DETECTOR

The output of a M-Z interferometer is described as

$$I(\omega_m, t) = \frac{1}{2}I_o\left[1 + \cos\left\{\frac{\pi}{2}M(\omega_m)\frac{V_d(t)}{V_\pi} + \phi_o\right\}\right] \tag{B.1}$$

where

$$V_d(t) = V_s G(t)\cos\omega_m t \tag{B.2}$$

$V_d(t)$ is the driving voltage incurring the electrooptic effect. V_s is the swing voltage of the gate function that modulates again the MW signal. $G(t)$ is the gate function of 1 kHz with unit amplitude. $M(\omega_m)$ is the factor by which the effective influence on phase retardation at ω_m is taken into consideration. Substitution of Eq. (B2) into Eq. (B1) gives

$$I(\omega_m, t) = \frac{1}{2}I_o\left[1 + \cos(\chi\cos\omega_m t + \phi_o)\right] \tag{B.3}$$

where

$$\chi = \frac{\pi}{2}M(\omega_m)\frac{V_s}{V_\pi}G(t) \quad \left(\frac{V_s}{V_\pi} \ll 1\right) \tag{B.4}$$

Eq. (B3) is expanded in terms of Bessel functions as

$$\begin{aligned} I(\omega_m, t) = {} & \frac{1}{2}I_o + \frac{1}{2}I_o cos\phi_o J_o(\chi) \\ & + I_o\sum_{n=1}^{\infty}(-1)^n\Big\{-\sin\phi_o J_{2n-1}(\chi)\cos(2n-1)\omega_m t + \cos\phi_o J_{2n}(\chi)\cos 2n\omega_m t\Big\} \end{aligned} \tag{B.5}$$

For $V_d(t) = 0$, ϕ_0, a bias-related parameter, is adjusted so that $I(\omega_m, t)$ becomes 0. For the case of Eq. (B1), ϕ_0 needs to be set to π.

Eq. (B5) may be approximated as below when $\chi \ll 1$.

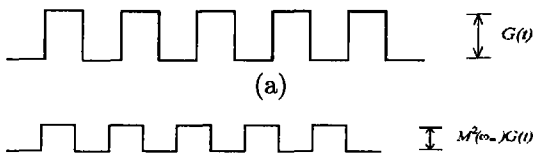

FIG. 6. Amplitude variation of 1 kHz Gate function with respect to ω_m. (a) $\omega_m = 0$ (b)$\omega_m \neq 0$.

$$I(\omega_m, t) \simeq \frac{1}{2} I_o - \frac{1}{2} I_o (1 - \frac{\chi^2}{4}) + I_o \sum_{n=1}^{\infty} c_n J_n(\chi) \cos n\omega_m t \qquad \text{(B.6)}$$

The cosine terms of Eq. (B6) represents the harmonic frequency of driving MW signal. These terms are detected by a low-speed detector, averaging to 0.

When the modulated MW voltage $V_s G(t) \cos \omega_m t$ is applied on the electrode, the optical intensity detected by the low-speed detector are now

$$I(0,t) = \frac{1}{8} I_o \left(\frac{\pi}{2} \frac{V_s}{V_\pi} \right)^2 G(t) \propto G(t) \qquad \text{(B.7)}$$

$$I(\omega_m, t) = \frac{1}{8} I_o \left(\frac{\pi}{2} \frac{V_s}{V_\pi} \right)^2 G(t) M^2(\omega_m) \propto M^2(\omega_m) G(t) \qquad \text{(B.8)}$$

Typical wave forms of Eqs. (B7) and (B8) are depicted in Fig. 6.

The optical response is defined as the square root of a ratio of output intensities.

$$R(\omega_m) = \sqrt{\frac{I(\omega_m, t)}{I(0,t)}} = M(\omega_m) \qquad \text{(B.9)}$$

$I(\omega_m, t)$ is converted to current form or voltage form through optical detectors by the square-law, which form is to be displayed in an oscilloscope. In this respect, $R(\omega_m)$ is defined in two ways as such [10] 20 log $R(\omega_m)$: dB-optical and 20 log $R^2(\omega_m)$: dB-electrical.

*Corresponding author : cmkim@uoscc.uos.ac.kr.

REFERENCES

[1] D. W. Dolfi and T. R. Ranganath, Electron. Lett., **28**, 1197 (1992).
[2] G. K. Gopalakrishnan, C. H. Bulmer, W. K. Burns, R. W. McElhanon, and A. S. Greenblatt, Electron. Lett., **28**, 826 (1992).
[3] S. K. Korotky, G. Eisenstein, R. S. Tucker, J. J. Veselka, and G. Raybon, Appl. Phys. Lett., **50**, 1631 (1987).
[4] R. E. Tench, J.-M. P. Delavaux, L. D. Tzeng, R. W. Smith, L. L. Buhl, and R. C. Alferness, J. Lightwave Technol., **LT-5**, 492 (1987).
[5] R. Spickermann and N. Dagli, IEEE Trans. Microwave Theory Tech., **42**, 1918 (1994).
[6] K. Noguchi, O. Mitomi, H. Miyazawa, and S. Seki, J. Lightwave Technol., **13**, 1164 (1995).
[7] K. Noguchi, O. Mitomi, and H. Miyazawa, J. Lightwave Technol., **16**, 615 (1998).
[8] R. C. Alferness, S. K. Korotky, and E. A. Marcatili, IEEE J. Quantum Electron., **QE-20**, 301 (1984).
[9] G. K. Gopalakrishman, W. K. Burns, R. W. McElhanon, and A. S. Greenblatt, J. Lightwave Technol., **12**, 1807 (1994).
[10] K. W. Hui, K.. S. Chiang, B. Wu, and A. H. Zhang, J. Lightwave Technol., **16**, 232 (1994).
[11] S. Uehara, Appl. Opt., **17**, 68 (1978).
[12] M. Nazarathy, D. W. Dolfi, and R. J. Jungerman, J. Lightwave Technol., **LT-5**, (1987).
[13] K. Kubota, J. Noda, and O. Mikami, IEEE J. Quantum Electron., **QE-16**, 754 (1980).
[14] D. Erasme, M. G. F. Wilson, Optical & Quantum Electron., **18**, 203 (1986).
[15] W. Wang, R. Tavlykaev, and R. V. Ramaswamy, IEEE J. Photon. Technol. Lett., **9**, 610 (1997).
[16] C. H. Bulmer, W. K. Burns, and C. W. Pickett, IEEE Photon. Technol. Lett., **3**, 28 (1991).